Fatigue Strengthening of Steel Bridges with Adhesively Bonded CFRP Laminates: Case Study

Sylvain Chataigner, Mazen Whabeh, David Garcia Sanchez, Karim Benzarti, Veit Birtel, Mickael Fischer, Luis Sopena, Rami Boundouki, Frank Lehmann, Elena Martin, et al.

Journal of Composites for construction, ASCE, 24, 3 (2020)
https://doi.org/10.1061/(ASCE)CC.1943-5614.0001014

Fatigue strengthening of steel bridges with adhesively bonded CFRP laminates: case study

S. Chataigner[1],M. Wahbeh[2], D. Garcia-Sanchez[3], K. Benzarti[4], V. Birtel[5], M. Fischer[6], L. Sopena[7], R. Boundouki[8], F. Lehmann[9], E. Martin[10], G. Gemignani[11], M. Zalbide[12]

[1] Senior Researcher, IFSTTAR, MAST, SMC, Route de Bouaye, F-44344 Bouguenais, France (sylvain.chataigner@ifsttar.fr)

[2] Executive Chairman, Alta Vista Solutions, 3260 Blume Dr., Suite 500, Richmond, CA 94806, USA (mwahbeh@altavistasolutions.com)

[3] Senior Researcher, TECNALIA, Parque Tecnologico de Bizkaia, E-48160 Derio – Bizkaia, Spain (david.garciasanchez@tecnalia.com)

[4] Director of Research, Université Paris-Est, Laboratoire Navier (UMR 8205), IFSTTAR, Ecole des Ponts ParisTech, Cité Descartes, F-77447 Marne La Vallée, France (karim.benzarti@ifsttar.fr)

[5] Senior researcher, MPA, Materials Testing Institute University of Stuttgart, Pfaffenwaldring 4, 70569 Stuttgart, Germany (veit.birtel@mpa.uni-stuttgart.de)

[6] Project manager, Leonhardt, Andrä und Partner Beratende Ingenieure VBI AG (LAP), Rosenthaler Strabe 40/41, Berlin, Germany (Michael.fischer@lap-consult.com)

[7] Project manager, Dragados S.A., Avda Camino de Santiago 50, 28050 Madrid, Spain (lsopenac@ggravityeng.com)

[8] Vice President, Alta Vista Solutions, 57 W, 57th Street, NY 10 019, USA (rboundouki@altavistasolutions.com)

[9] Senior researcher, MPA, Materials Testing Institute University of Stuttgart, Pfaffenwaldring 4, 70569 Stuttgart, Germany (frank.lehmann@mpa.uni-stuttgart.de)

[10] Head of Innovation Projects, Dragados S.A., Avda Camino de Santiago 50, 28050 Madrid, Spain (emartind@dragados.com)

[11] *Project manager, Collanti Concorde, Via Schiaparelli, 12 - Z.I., 31029 Vittorio Veneto, Italy (gianluca.gemignani@collanticoncorde.it)*

[12] *Project coordinator, TECNALIA, Parque Tecnologico de Bizkaia, E-48160 Derio – Bizkaia, Spain (maria.zalbide@tecnalia.com)*

ABSTRACT

One of the goals of applying sustainable development to bridge infrastructure is to provide bridge owners with strengthening solutions that may lead to increased service life for existing structures. In the case of steel bridges, assessment of the remaining service life is most often linked to the determination of structural deterioration caused by corrosion and fatigue. Damage caused by fatigue is very difficult to assess before crack initiation, and is more likely to occur in old structures, for which the phenomenon was not taken into account in designs before 1970. In addition, old steel materials display more brittle behaviour. In answer to these challenges, a preventive methodology for fatigue strengthening of steel structures was developed. The method begins with scheduling a fatigue design analysis of the existing construction to determine the most fatigue damage exposed construction elements of the bridge. The remaining fatigue life of these elements can be increased with a strengthening solution based on the use of adhesively bonded ultra high modulus (UHM) carbon fibre-reinforced polymer (CFRP) plates, which is applied to a steel surface before failure indicators such as cracks arise. This article presents the development process of this preventive method and a demonstrative application to an existing bridge (Jarama Bridge). Strain measurement was carried out to verify the theoretical expectations of the reinforcement. Different parameters were studied, including the influence of low traffic volumes during reinforcement application. The results proved the efficiency of this system for the structure under study.

Key words: Strengthening, fatigue, steel bridges, CFRP composites, on-site application, life extension.

Introduction

There is a strong need worldwide to develop and assess sustainable solutions to increase the life expectancy of existing infrastructure. This is particularly true in the case of steel bridges both in Europe and in the USA (Lee 2012) (Ye et al. 2014). Most of these structures were constructed according to old standards in which fatigue was not considered, despite fatigue being the second main pathology after corrosion affecting steel structures (Palmer 2014). Most of the bridges of concern are approaching the end of their designed service life. In addition, they have often been subjected to traffic substantially above the amount anticipated most likely significantly decreasing their life expectancy (Kühn et al. 2008). To date, the mainstream approach against fatigue problems was centred on a reactive strategy based on maintenance or repair operations undertaken after the occurrence of cracks in the structure. With an aging bridge stock, it is necessary to change this paradigm and widely adopt a preventive strategy. Ultimately this approach will support a more sustainable management of life expectancy of steel structures (Ghafoori 2019) (Orcesi et al. 2019).

Existing reinforcement or repair methods for steel structures are mostly based on the installation of additional steel plates attached either by riveting, bolting or welding (FHWA 2013). These methods have the disadvantage of adding a large additional weight, are difficult to implement (labour-intensive and disruptive to traffic), and may decrease fatigue life expectancy due to local stress concentrations in the connection areas (Karbhari 2014). Carbon Fibre-Reinforced Polymer (CFRP) composites, though more expensive than steel plates, present several relevant advantages making them suitable and cost effective for steel bridge retrofitting. Research has already proven the efficiency of CFRP composites particularly with regards to fatigue (Dawood et al. 2007) (Kim et al. 2011) (Kamruzzaman 2014). CFRP installation is less time consuming as compared to traditional repair solutions;, typically a few days to a month, therefore causing fewer traffic disruptions (Peiris 2015). Such composite materials additionally exhibit a high strength-to-weight ratio, excellent fatigue properties, and high durability and versatility, and are easy to handle and apply without the need of heavy equipment (Miller et al. 2001) (Tavakkolizadeh et al. 2003) (Zhao et al. 2007) (Bocciarelli et al. 2008). Their attachment to the existing

structure can be achieved either by adhesive bonding or by using frictional equipment (Kianmofrad et al. 2017). A number of guidelines have been recommended to ensure improved quality of CFRP installation on steel structures (Moy 2001) (Cadei et al. 2004) (Schnerch et al. 2007) (CNR 2007) (DNV 2012). Previous investigations identified two main options for the design of cost-effective CFRP strengthening systems to be applied to steel structures (Ghafoori et al. 2015a): Ultra High Modulus (UHM) CFRP reinforcement (Schnerch et al. 2007) or prestressed CFRP composite plates (Ghafoori et al. 2015b) (Ghafoori et al. 2016). Since the first documented application of adhesively bonded CFRP reinforcements for the strengthening of the Tickford Bridge in the UK (Lane et al. 2000), only a small number of on-site demonstration projects have been reported in literature (Miller et al. 2001) (Luke 2001) (Hollaway et al. 2002) (Moy et al. 2007) (Zhao 2013) (Moy 2014) (Peiris et al. 2015) (Ghafoori et al. 2015c) (Ghafoori et al. 2018). Disappointingly, the actual use of application of adhesively bonded CFRP reinforcements to civil steel structures remains limited.

Recently, a preventive strategy regarding fatigue of steel structures, relying on the use of adhesively bonded CFRP reinforcement, was developed (Wahbeh et al. 2018 a). This strategy relies mostly on a precise diagnosis of the structure, a remaining fatigue assessment methodology, and a specific adhesively bonded reinforcement process based on the use of a commercially available UHM CFRP plate combined with a novel formulated polymer adhesive intended to provide enhanced adhesion on steel substrates and improved resistance to fatigue, humidity aging and high temperatures (Chataigner et al. 2018). Of course, due to the fixed shape and the high stiffness of the UHM CFRP plate, such a reinforcement solution is only adapted to plane surfaces and is not compliant with non-planar critical details (Hu et al. 2017). The whole methodology was applied on an actual steel bridge, the Jarama Bridge, which is presented herein.

The first section of this article aims to describe the steel bridge on which the methodology was applied, in order to demonstrate and assess the process. The second portion is devoted to the application of the developed methodology to this structure. This includes its preliminary diagnosis, the initial residual life assessment, a short description of the reinforcement system, and the design of the reinforcement. The

third section addresses the field application of the solution and the monitoring used to assess its efficiency. In the last section, the realized load tests and their results are presented and discussed.

Presentation of the studied steel bridge

General overview

The Jarama Bridge is a five-span steel bridge carrying two lanes of traffic on Road M-111 over the Jarama River in Madrid, Spain, connecting the Barajas-Madrid Airport to Paracuellos de Jarama. The bridge has a central three-span continuous segment and two simple side-span segments (figures 1 and 2). The bridge superstructure consists of two main longitudinal built-up I-section steel plate girders with transverse cross-bracing and floor beams. The two main girders were partially pre-fabricated and finally assembled and welded in the field. The connections between the main girders and additional steel elements (e.g. cross-bracing, floor beams) were assembled and welded on-site. The deck of the bridge consists of a non-composite concrete slab simply supported by the steel girders. The girders are supported by neoprene bearings on the abutments, and fixed and movable steel plate bearings on the piers.

The bridge was designed in 1962 following the 1956 Spanish Design Code, and was built around 1965 to replace the old bridge over the Jarama River. Existing bridge plans and documentation show that the main structural elements were manufactured using F-622 steel (UNE 1981). The material properties of the F-622 steel were similar to the A-42B steel and comparable to the actual S-275 steel with an elastic limit of 255 MPa and rupture strength between 410-520 MPa. The top and bottom flanges of the main I-shaped girders in the central continuous spans have a width of 700 mm and a thickness of 30 mm. The girder web thickness is 15 mm, while the height varies between 1,870 mm and 2,810 mm. The girders in the simply supported spans have 200×45 mm flanges and 1,870×12 mm webs.

The steel elements of the Jarama Bridge were generally in a good condition. However there was evidence of local deficiencies including moisture, moss, corrosion. On the top flange of the main girders, general corrosion was noted. In some cases, the corrosion had already progressed into the web plates. In other cases, efflorescence and peeling problems were discovered. The same deficiencies were also present on the bottom flange. Crosses or x-bracing appeared to be in good condition and had no visual defects. Moreover the bottom lateral bracing members of span 1 showed obvious distortion, corrosion and other defects probably caused by the impact of objects. One angle in the bottom lateral bracing member of span 5 also presented a small deformation.

The floor beams were in good condition. Moisture, efflorescence and corrosion on the top flange were noted locally. Some areas of damaged and peeled coating could be seen in the bottom flange. Larger areas affected by moisture and corrosion were located in the floor beams over piers and abutments.

Specific issues regarding material characterization and fatigue

The bridge design did not incorporate any fatigue criteria since there were no fatigue requirements in the 1956 code. However, the structural steel elements were designed with a tension limit of 137 N/mm^2 which correspond approximately to a 1.80 safety factor—the most conservative safety factor according to the 1956 design code—to cover all effects.

The prefabricated sections of the main steel girders were initially welded at the workshop and then transported to the job site, where they were assembled and welded in place. Overall, a total of 36 butt-welded joints were welded in the factory, and another eight field butt-welded joints were welded on-site on both main girders. The resulting stress concentrations in the butt-welded splices can produce a reduction in the fatigue capacity of the girders. The presence of these fatigue-prone details in the main girders makes the Jarama Bridge a suitable candidate structure for implementation of a preventive fatigue strengthening of steel structures with adhesively bonded CFRPs. As part of the proposed retrofit, a detailed bridge inspection was performed on the Jarama Bridge in 2017; visual inspections and

nondestructive tests (i.e. ultrasonic tests) were performed on four on-site butt-welded splices and 27 splices welded in the factory. Results from the visual inspections and ultrasonic tests showed that the selected on-site welds did not comply with the quality standards according to AL2 (UNE 2011) or level B (UNE 2014). Level B means that there are high-level imperfections, and level AL2 is an ultrasonic acceptance level for full penetration welded joints in ferritic steels corresponding to level B quality according to CEN (2014). Eleven of the in-shop welds also failed to meet the quality standards under AL2. These observations, summarized in Table 1, conclude definitively that the on-site and in-shop butt-welded splices do not meet current quality standards. This is not surprising given the advancement in bridge welding codes and improved implementation over the past 50 years.

Eight steel test coupons taken from girders have been tested for material characterization, including mechanical, chemical and metallographic examination. Chemical and metallographic results show that none of the test coupons meet the standards of F-622 classification with accordance to CSIC (1969), nor A-42b characteristics with standards (COAM 1964). During evaluations in accordance with UNE (2006), six tested coupons met the quality standards and only two did not. A tensile strength test, Brinell hardness test and Charpy impact test were also performed. Four test coupons were obtained from the transverse stiffener of girders. All of them met F-622 characteristics in accordance with CSIC (1969), A-42 b in accordance with standards from COAM (1964), S235JR and S275JR in accordance to UNE (2006). Four more coupons were cut out from the bottom flange of the girders. One of them met the characteristics of F-622 and A-42ba. Two of them meet S235JR quality in accordance with UNE (2006). The remainder of the test coupons did not meet any quality requirements.

Description of the proposed methodology to prevent fatigue damage

Preliminary diagnosis of the structure

192 The most critical locations regarding fatigue of steel structures are the assembly joints (Kühn 2008)
193 (FHWA 2013) (Palmer 2014). As the presented application is part of a demonstration, only eight shop
194 butt-welds on both main steel girders in one of the central spans (span 2) were considered adequate (no
195 defects, easy access) and initially selected to be strengthened using the developed adhesively bonded
196 CRFP reinforcement. However, because of the proximity of two of these pre-selected welds to the kink
197 of the bottom flange, it was decided to exclude them from the investigation. Figure 3 shows the location
198 of the six shop butt-welds (welds 29, 26, 25, 20, 17, and 16) that were strengthened and evaluated in
199 this investigation. An additional denomination of those six locations is also used in this document in
200 order to remind the span (S), beam (B) and weld (W) locations. Thus, the weld n°29 is also denominated
201 S2-B1-W1 as it is the first butt weld located on the first beam of the second span. The correspondence
202 between weld number and this identification is reminded for each of the six studied welds in Figure 3.
203
204 Obviously, in the case of an actual bridge requiring full evaluation, the entire structure should be
205 analyzed and the assessment of residual service life determined for each element and joint. This would
206 allow identification of the most critical locations in need of reinforcement.
207
208 ***Assessment of residual fatigue life***
209
210 The fatigue resistance and remaining fatigue life of the remaining girders were estimated using the
211 FASSTbridge fatigue assessment methodology that had been developed to provide a reliable and
212 preventive fatigue assessment of existing steel bridges in a pre-failure condition, and calculate the life-
213 time expectancy (Wahbeh et al. 2018b) (Figure 4). The FASSTbridge fatigue assessment tool was
214 developed based on both AASHTO (AASHTO 2012) and Eurocode (CEN 2002) specifications and
215 consist of a questionnaire purposely created to gather both quantitative and qualitative information about
216 the bridge and the specific detail being analyzed. In this approach, the questionnaire inputs have been
217 limited to pre-determined values in order to generate a set of modification factors (α values) for different
218 fatigue design variables, and to perform the required fatigue assessment calculations. Table 2 and Table

3 summarize the fatigue design variables based on AASHTO and Eurocode specifications and corresponding proposed modification factors (α values).

The estimation of fatigue capacity and remaining fatigue lifetime were performed according to the Eurocode recommendations. The results for the six studied locations are shown in Table 4. These results highlight that only one of the studied locations seems to be critical regarding fatigue (which is consistent with the real status of the bridge: no fatigue damage detected). Yet, in order to study the efficiency of the reinforcement and to investigate different application parameters, it was decided to apply the developed reinforcement on all six locations.

Description of the strengthening system

The developed strengthening system relies on the use of a commercial UHM CFRP plate provided by Epsilon Composite (France). A specific bi-component hybrid epoxy/polyurethane adhesive was developed for this application by Collanti Concorde (Italy). In order to obtain the required specification of glass transition temperature $T_g > 71°C$, which is at least 15°C above the maximum service temperature expected on steel bridges in Europe (CEN 2002), this adhesive needs to be post-cured after application at 80°C for one hour. An extensive experimental program enabled the whole system behavior to be checked, including determining its design characteristics, its sensitivity and replicability, its dependency to temperature, and its durability both regarding moisture and fatigue. More details on these issues can be found in Chataigner et al. (2018).

Design of the reinforcement

Three different CRFP strengthening configurations with a varying numbers of CFRP plates, numbers of layers, and lengths were evaluated. A maximum of five CFRP plates per weld were selected based on the width of the girder bottom flange and a 30 mm minimum separation between consecutive CFRP plates. A minimum length of 1,200 mm was adopted for the CFRP plates. This allows for covering of

247 the butt weld to reinforce (200 mm) including twice the required anchorage length of 120 mm
248 determined in Chataigner et al. (2018), and an additional safety length in order to cope with the creep
249 of anchorage length with aging (380 mm on each side).
250
251 A preliminary investigation of the effects of the geometry of CFRP plates indicated the influence of the
252 sheet length is negligible provided it is superior to the characteristic anchorage length (Nozaka et al.
253 2005). Using a CFRP plate with a length of 1,200 mm led to similar results as employing a CFRP plate
254 over a longer span for the considered application of this study (localized butt weld reinforcements). In
255 this preliminary analysis, it was assumed only normal longitudinal stresses were present in the section
256 and the CFRP and steel would act compositely as a one unit.
257
258 For the strengthening configurations with several layers of CFRP plates, an additional anchorage length
259 of 100 mm was added to each end of the CFRP panel. Details of all six strengthening configurations
260 evaluated in this investigation are summarized in Table 5 and Figure 5. Each of the CFRP plates
261 employed in all strengthening configurations had a thickness of 4.0 mm, a width of 100 mm, and a
262 modulus of elasticity of 460,000 N/mm^2. The investigations in Chataigner et al. (2018) were used to
263 extrapolate the ultimate acceptable stresses within the applied reinforcement (1,074 microstrain for one-
264 layer configuration, 537 microstrains for two-layer configuration, and 358 microstrains for three-layer
265 configuration). Taking into account the fatigue resistance of the adhesively bonded assembly, it was
266 necessary to adopt 30% of this ultimate value in service to ensure a fatigue level under the fatigue
267 endurance limit.
268
269 To evaluate the performance of each strengthening configuration with CFRP plates on butt welds, a
270 series of finite element analyses (FEAs) were conducted in order to obtain the differences between the
271 minimum and maximum stresses in the six butt welds due to fatigue loading for the reference
272 (unstrengthened) and strengthened structural configurations (Diez et al. 2017). As expected, there was
273 a correlation between the reduction in the tensile stresses in the welds and the number of layers and

CFRP plates. As the number of layers and the number of CFRP plates installed increased, larger reductions on the stress ranges were observed.

For the strengthening configuration of four CFRP plates and two layers per weld, a reduction of approximately 8-15% in the stresses were achieved. When five CFRP sheets were used in a single layer configuration, a 4-7% reduction in the stresses in the weld were estimated. The largest reduction of approximately 21% was achieved with a strengthening configuration using three CFRP plates in three layers.

Based on these results, the remaining fatigue life has been determined for the six studied locations for the strengthened situation using a finite element to obtain stress reduction and the developed remaining fatigue life tool (Wahbeh et al. 2018 b). This fatigue assessment tool was developed according to NCHRP (2012) through a simple questionnaire for bridge owners which takes into account several parameters on fatigue class details such as state of damage or real traffic loads. The results from the studied details are presented in Table 6. For the only critical location (Weld N° 17), the remaining fatigue life seems to be almost tripled due to the reinforcement, indicating the efficiency of the proposed solution.

Application of the strengthening solution in the field

Installation of CFRP systems

The installation of the bonded reinforcement was carried out according to the recommendations of Schnerch et al. (2007) and Italian National Research Council (CNR 2007). Prior to installation of the CFRP plates, the steel surface was initially grit blasted to remove coatings (painting), corrosion products, and any other particles that could affect the bond properties between the CFRP adhesive and the steel. In the case of lead paint, as is often encountered in old steel structures, this process may require extensive protective measures during surface preparation operations. In the case of Jarama Bridge, this

was not the case, and classical methodologies could therefore be adopted. The surface preparation was performed following CEN (2007), to achieve a level of Sa 2 1⁄2 required for the system. The welds were also grinded to eliminate any geometric disruptions in the weld and obtain a flat surface. After grit blasting and weld grinding, the entire steel surface was cleaned and degreased.

The CFRP plates are up to 1,600 mm long, 4-mm thick, and up to three layers, as previously reported in Table 5. The material is UHM CFRP (E = 460 GPa). Because the stiffness of the CFRP plates is relatively high, and even more so when applied in several layers, the adaptability of the plates to the geometry of the steel plates is very low, and therefore any geometric deviations from a plane (both longitudinal and transverse) or other irregularities must be accommodated by the adhesive. The thickness of the adhesive was measured and found to be at least one mm; analysis and tests indicated no reduction of capacity for thicknesses up to 3 mm (Chataigner et al. 2018). For each CFRP plate, a 45° tapering was carried out on each edge as recommended in Schnerch et al. (2007).

In the case of the Jarama Bridge, it was decided to retrofit the bottom flange of the girders which are in tension and therefore susceptible to fatigue cycles. Since the CFRP plates are to be installed underneath the girders, it was necessary to use a fixation system that would be able to keep the plates in place during the curing and hardening of the adhesive. First, the adhesive mix was applied directly to the surface of the CFRP plate after removal of the peel-ply. To spread the adhesive uniformly, a device similar to a trowel with a v-notch was used (Figure 6a). In the case of the multi-layer configurations, the prefabrication option was selected. Previously, at the workshop or on-site, the layers were attached to each other in the predefined arrangement, and pressure was then applied with small rollers to ensure all air bubbles or gaps were removed (Figure 6b). The CFRP plate with the adhesive on one side must be pressed into the steel starting from one end and gradually moving towards the other to allow air to escape. A laminate roller was used from the center of the plate towards the ends to remove as much air as possible and ensure good contact between the CFRP, adhesive and steel substrate. The excess resin that escaped during pressing was removed, leaving a 45° fillet as recommended in Schnerch et al. (2007). Care was taken to ensure that not too much adhesive would be pressed out from the joint at the plate

ends, and that the adhesive thickness in the end regions was consistent with the rest of the plate. Once the CFRP, adhesive and steel surface were completely in contact, the plates were clamped to the steel structure with the fixation system developed *ad hoc*.

As described in Chataigner et al. (2018), a post-curing of the system is needed (one hour at 80 °C) in order for the adhesive's glass transition temperature to reach the required value of 71 °C without losing properties. Ceramic pads were used to transfer the heat to the system to reach the target curing temperature of 80 °C and maintain it constant during the curing time (one hour). The ceramic pads were placed to completely cover the surface of the CFRP plates (Figure 7). Thermocouples were installed on the steel surface close to the CFRP plates and were used to control the curing temperature. Isolation blankets were also used to reduce heat loss, maintain the required temperature inside the system, and improve energy efficiency. The post-curing process started a minimum of two hours after installation of the CFRP plates.

After removal of the heating system, paint was applied to the whole reinforcement and surrounding steel to protect the area where the coatings had been removed. The selected coating had been previously assessed through experimental investigations to ensure its compatibility with both the steel surface and CFRP plates.

Each of the six weld locations were reinforced during nighttime to reduce traffic disruptions. The duration of the application (including post-curing) lasted between 4.5 to 6.5 hours, depending on the precise weld location and CFRP configuration, and the influence of the learning curve for the installation. For three locations (welds n°17, 20 and 25), traffic was partially deviated during the entire application (only one traffic lane open instead of two lanes). For two locations (welds n°26 and 29), traffic was deviated only during the application of the bonded CFRP plates before post-curing. For one of the locations (weld n° 16), traffic was not deviated at all.

Description of the monitoring instrumentation

Before applying the reinforcement, electro-mechanic strain gauges were installed at the six studied locations. For each location, four strain gauges were installed on top of the bottom flange in the longitudinal direction. A first pair of strain gauges was installed 80 mm from the studied butt weld. One of the gauges was bonded to the flange, while the second was bonded to a separate piece of metal to compensate for temperature effects due to a half-bridge circuit (Figure 8). The second pair was installed 950 mm from the studied butt weld, outside of the reinforced zone. The denomination of the strain gauges in the rest of the article will be X-1 and X-2, corresponding respectively to the first axial strain at 80 mm from the studied weld and the second axial strain at 950 mm from the studied weld, and X corresponding the weld number. The strain gauges received a silicone protective cover to shield them from adventitious mechanical interaction (i.e. impact, bump) during the strengthening intervention. An HBM Spider8 data acquisition system with a 200 Hz measurement rate was used, which allowed the simultaneous recording of all 12 half-bridge circuits. All strain data were recorded with reference to the bridge state without traffic loads ("differential strain"). "Positive" strains correspond to additional tension, while "negative" strains correspond to reduced tension in the girders with respect to the initial condition.

A recently developed debonding sensor was also installed during the application of the CFRP reinforcement. It is described in detail in Lehmann et al. (2019). This debonding sensor was installed during the strengthening intervention in order to verify its applicability. It consists of an ultra-thin square element that needs to be inserted into the bond line close to the edge (Figure 9). Preliminary laboratory experimental investigations confirmed the insertion of this sensor did not induce premature debonding (Lehmann et al. 2019). No difficulty was encountered during the application onsite, and no debonding was detected during any of the led investigations. The sensors will need to be investigated at a later date to verify whether debonding occurred during the structure's service life.

Efficiency assessment of the reinforcement

Description of the bridge loading tests

A fixed load test was performed in order to gain knowledge about the condition of the Jarama Bridge. By measuring strains both before and after the bridge retrofit, this fixed load condition test was able to effectively demonstrate the effectiveness of the intervention. The tests took place during the two nights immediately before and after the retrofitting. All of the load tests were repeated for both lanes on the bridge even when one lane had to be blocked.

First, a static fixed load test was performed including three different truck positions. The static test was performed by placing two 27-ton trucks (Renault Kerax) in three predefined positions (Figure 10), carrying out the strain measurements after stabilizing the load. The initial position was chosen to obtain maximum strains in welds 17, 20, 26 and 29. The second position was chosen to obtain maximum positive strains in welds 16, 17, 25 and 26. The third position was chosen to obtain maximum negative strains in the studied welds.

Two dynamic load tests were then performed by placing a wooden plank, four cm in height, in two selected positions, over which a single truck passed at speeds of 20 km/h and 50 km/h (Figure 11). The passage of the truck when hitting the plank induced a vertical dynamic impact load in the structure. No take-off and break loading scenarios were carried out in the presented case, although these may also have a strong impact on the measured stresses as detailed in (Hosseini et al. 2019), due to its potential to increase the static stresses measurements from 50%.

Obtained results and discussion

An example of strain recording during the positioning of the two trucks on the bridge for a static load test is provided in Figure 12 (the first position load case is given in figure 10). As anticipated, the first studied position, welds 20, 29, 26 and 17 are subject to the highest strain. Since only one side of the bridge was blocked to traffic, there are some small perturbations of the measurement due to the traffic

on the other side. However, as the plateau value is considered, these perturbations do not affect the obtained results. For each weld location, the maximum measured differential strains before and after reinforcement are provided in tables 7 and 8.

An example of strain recorded during the dynamic load tests is provided in Figure 13. A clear dynamic effect may be observed as the strain levels reached are almost as high as those obtained in static tests, though the applied load is half as high. Furthermore, the speed of the truck had a slight effect on the results, resulting in an increase in the dynamic effect. For each weld location, the maximum measured differential strains before and after reinforcement obtained during dynamic tests are also provided in tables 7 and 8.

For each of the six locations, strains were reduced thanks to the CFRP reinforcement both close to the weld toe (Table 7) and far from the weld toe (Table 8). This experimentally observed reduction seems to be higher than the theoretically anticipated reduction through FEA. This was attributed to a local bending effect due to the asymmetric reinforcement geometry. This also explains the observed strain reduction on the second location (X-2) situated far from the weld toe, although it was situated outside the reinforced area. Static and dynamic results appeared to be very similar except for weld 26.

As the most critical fatigue zone is the location close to the weld (X-1), corresponding strain measurements are represented in Figure 14. The highest strain reductions (20 to 30 %) were obtained for locations reinforced with the highest number of CFRP plates, and the proposed solution worked well in the case of the three-layer configuration (welds 16 and 25). In addition, there was no discrepancy in the locations reinforced without total traffic disruption (welds 16, 26 and 29). This suggests that the proposed solution could be applied under low traffic, which would be a critical advantage of this strengthening method.

Conclusions

As far as the fatigue of steel structures is concerned, most of the time, structure owners employ a curative strategy after the detection of cracks in the most critical details. The presented application is aimed at highlighting the possibility of utilizing a preventive strategy before fatigue crack initiation to increase the lifetime of steel structures. From this demonstration on the Jarama Bridge in Madrid, Spain, several conclusions were obtained:

- The developed fatigue assessment methodology allowed for identification of the most critical locations and assessment of the remaining service life of the studied details. This is a key step of the proposed methodology and requires a precise study of the structure and details in question. In the case of old steel structures, it is often very difficult to meet the requirements of existing standards. This may introduce additional difficulties to the assessment process.
- As assembly details are the most critical components in fatigue, the applied reinforcement is highly localized. This allows for use of adhesively bonded reinforcement processes that require post-curing. Although such an operation was successfully applied here at real scale, there may be alternative post-curing systems which could improve the application (reduce complexity and cost). It could also be interesting to keep developing an adhesive which does not need post curing, or define the boundary conditions where the post-curing would not need to be necessary. The efficiency of stress transfer was demonstrated through the strain measurements.
- There seems to be no effect for the studied case when reinforcing the critical detail under traffic loads. This should be more deeply studied, especially if higher service strains are encountered, but offers interesting perspectives in terms of usage constraints, avoiding traffic deviation and closures (Orcesi et al. 2019).
- The strain measurement allowed for verification of the efficiency of the reinforcement system for both static and dynamic loading and for the three different reinforcement configurations. A 20 to 30% stress decrease was accomplished, allowing for an increase in the remaining service life for the most critical detail (more than double). The measured stress decrease was slightly higher than what was expected. This may be due to local bending effects.

  In addition, the onsite strain measurement resulted in noting CFRP strains were much smaller than the design strains determined through preliminary laboratory investigations.

Acknowledgements

The authors wish to acknowledge Epsilon Composite for supporting this study.

This work is part of the FASSTBRIDGE project. This project has received funding from the European Union's Seventh Framework Programme for research, technological development and demonstration under grant agreement no. 31109806.0008.

FASSTbridge is co-funded by Funding Partners of The ERA-NET as well as Infravation and the European Commission. The Funding Partners of the Infravation 2014 Call are:
Ministerie van Infrastructure en Milieu, Rijkswaterstaat, Bundesministerium für Verkehr, Bau und Stadtentwicklung, Danish Road Directorate, Satens Vegvesen Vegdirektoratet, Trafikverket – TRV, Vegaderdin, Ministère de l'Ecologie, du Développement Durable et de l'Energie, Centro para el Desarrollo Tecnologico Industrial, ANAS S.p.A., Netivei, Israel – National Transport Infrastructure Company Ltd, Federal Highway Administration USDOT.

Data availability

Some or all data, models, or code generated or used during the study are available from the corresponding author by request (material characterization results, residual life assessment, reinforcement design, on site load test results).

REFERENCES

AASHTO (American Association of State Highway and Transportation Officials). (2012). "AASHTO LRFD bridge design specifications". Washington, DC.

Bocciarelli, M., Colombi, P., Fava, G., and Poggi C. (2003). "Fatigue performance of tensile steel members strengthened with CFRP plates". *Compos. Struct.*, 87(4), 334–43.

Cadei, J.M.C., Stratford, J.T., Holloway, L.C., and Duckett, W.G. (2004). *Strengthening metallic structures using externally bonded fibre-reinforced polymers*. London: CIRIA, 2004.

CEN (European Committee for Standardization). (2002). *"*Eurocode - Basis of Structural Design*"*. *EN1990:2002*, Brussels.

CEN (European Committee for Standardization). (2007). "Preparation of steel substrates before application of paints and related products – Visual assessment of surface cleanliness – Part 1: Rust grades and preparation grades of uncoated steel substrates and of steel substrates after overall removal of previous coatings*"*. *EN ISO 8501-1:2007*, Brussels.

CEN (European Committee for Standardization). (2014). "Welding - Fusion-welded joints in steel, nickel, titanium and their alloys (beam welding excluded) - Quality levels for imperfections". *EN ISO 5817:2014*, Brussels.

Chataigner, S., Benzarti, K., Foret, G., Caron, J.F., Gemignani, G., Brugiolo, M., Calderon, I., Pinero, I., Birtel, V., and Lehmann, F. (2018). "Design and evaluation of an externally bonded CFRP reinforcement for the fatigue reinforcement of old steel structures", *Eng. Struct*., 177, 556-65.

CNR (National Research Council). (2007*). "*Guidelines for the design and construction of externally bonded FRP systems for strengthening existing structures*". CNR-DT-202/2005*, Rome.

COAM (Colegio Oficial de Arquitectos de Madrid). (1964). "Acero Laminado para estructuras de edificacion". *Normas MV 102/1964*.

CSIC (Instituto de la Construction y del Cemento "Eduardo Torroja"). (1969). "Instruccion E.M. 62 para estructuras de acero". *Instruccion E.M. 62*.

Dawood, M., Rizkalla, S., and Sumner, E. (2007). "Fatigue and overloading behaviour of steel-concrete composite flexural members strengthened with high modulus CFRP materials". *J. Compos. Constr.*, 11(6), 659-669.

Diez, J., Garcia Sanchez, D., Weidemüller, M., Lehmann, F., Wahbeh, M., Boundouki, R., Sopena, L., and Iborra, C. (2017). *Implementation of FASSTbridge methodology: bridge service life recalculation and strengthening design*. Report D5.2, FASSTBridge, 54 p.

DNV (Det Norske Veritas). (2012). *RP-C301, Design, fabrication, operation and qualification of bonded steel repair of steel structures*.

FHWA (Federal Highway Administration). (2013). *Manual for Repair and Retrofit of Fatigue Cracks in Steel Bridges*. Publication No. FHWA-IF-13-020.

Ghafoori, E., Motavalli, M., Zhao, X.-L., Nussbaumer, A., and Fontana, M. (2015 a). "Fatigue design criteria for strengthening metallic beams with bonded CFRP plates". *Eng. Struct*., 101, 542–57.

Ghafoori, E., Motavalli, M., Nussbaumer, A., Herwig, A., Prinz, G.S., and Fontana M. (2015 b). "Determination of minimum CFRP pre-stress levels for fatigue crack prevention in retrofitted metallic beams". *Eng. Struct*., 84, 29–41.

Ghafoori, E., Motavalli, M., Nussbaumer, A., Herwig, A., Prinz, G.S., and Fontana, M. (2015c). "Design criterion for fatigue strengthening of riveted beams in a 120-year-old railway metallic bridge using pre-stressed CFRP plates". *Compos. Part B*, 68, 1-13.

Ghafoori, E., Motavalli, M. (2016). "A retrofit theory to prevent fatigue crack initiation in aging riveted bridges using carbon fiber-reinforced polymer materials". *Polymer*s, 8(8), 308-328.

Ghafoori, E., Hosseini, A., Al-Mahaidi, R., Zhao, X.L., and Motavalli, M. (2018). "Prestressed CFRP-strengthening and long-term wireless monitoring of an old roadway metallic bridge". *Eng. Struct.*, 176, 585-605.

Ghafoori, E. (2019). "Editorial for special issue on Sustainable Metallic Structures". *Eng. Struc.*, 183, 83.

Hollaway, L.C., and Cadei, J. (2002). "Progress in the technique of upgrading metallic structures with advanced polymer composites". *Prog. in Struct. Eng. and Mat.,* 4(2), 131-48.

545 Hosseini, A. Ghafoori, E., Al-Mahaidi, R., Zhao, X.L., and Motavalli, M. (2019). "Strengthening of a
546 19th-century roadway metallic bridge using nonprestressed bonded and unprestressed unbonded CFRP
547 plates". *Constr Build. Mat.,* 209, 240-259.
548 Hu, L., Feng, P., and Zhao, X.L. (2017). "Fatigue design of CFRP strengthened steel members". *Thin*
549 *Walled Struct*., 119, 82–98.

550 Kamruzzaman, M., Jumaat, M.Z., Ramli Sulong, N.H., and Saiful Islam, A.B.M. (2014). "A review on
551 strengthening steel beams using FRP under fatigue". *The Sci. World J.*, Article ID 702537, 2014, 21 p.
552 Karbhari, V.M. (2014). *Rehabilitation of metallic civil infrastructures using fiber-reinforced polymer*
553 *(FRP) composites*. Woodhead Publishing.

554 Kianmofrad, F., Ghafoori, E., Elyasi, M., Motavalli, M., and Rahimian, M. (2017). "Strengthening of
555 metallic beams with different types of pre-stressed un-bonded retrofit systems". *Compos. Struct*., 159,
556 81–95.

557 Kim, Y.J., and Harries, K.A. (2011). "Fatigue behaviour of damaged steel beams repaired with CFRP
558 strips". *Eng. Struct.*, 33, 1491-1502.
559 Kühn, B., Lukic, M., Nussbaumer, A., Günther, H.P., Helmerich, R., Herion, S., et al. (2008).
560 *Assessment of existing steel structures: recommendations for estimation of remaining fatigue life*. Joint
561 Res Centre Rep.

562 Lane, I.R. and Ward, J.A. (2000). *Restoring Britain's bridge heritage*. Inst. Civ. Eng. South Wales
563 Association, Transport Engineering Group Award.

564 Lee, S.K. (2012). *Current state of bridge deterioration in the U.S*. Piscataway, New Jersey: Rutgers
565 University.

566 Lehmann, F., Chataigner, S., Birtel, V., Wang, J., and Konrad, O. (2019). "Development of a sensor for
567 monitoring mechanically stressed adhesive joints". *Constr Build. Mat.,* 227, article 116627.
568 Luke, S. (2001). "The use of carbon fibre plates for the strengthening of two metallic bridges of an
569 historic nature in the UK". *Proc. of the CICE 2001*, Hong Kong: FRP Composites in Civil Engineering,
570 975–83.

571 Miller, T.C., Chajes, M.J., Mertz, D.R., and Hastings, J.N. (2001). “Strengthening of a steel bridge
572 girder using CFRP plates”. *J Bridge Eng.*, 6(6), 514–22.

573 Moy, S. (2001). *ICE design and practice guides – FRP composites life extension and strengthening of*
574 *metallic structures*. London: Thomas Telford Publishing.

575 Moy, S.S.J., and Bloodworth, A.G. (2007). “Strengthening a steel bridge with CFRP composites.
576 Proceedings of the Institution of Civil Engineers“. *Struct. and Build.*, 160(2), 81-93.

577 Moy, S., 2014. (2014). “Strengthening of historic metallic structures using fibre-reinforced polymer
578 (FRP) composites“. In Rehabilitation of Metallic Civil Infrastructure Using Fiber Reinforced Polymer
579 (FRP) Composites, 406-29.

580 Nozaka K., Shield C.K., and Hajjar, J.F. (2005). “Effective bond length of Carbon-Fiber-Reinforced
581 Polymer strips bonded to fatigued steel bridge I-girders”. *J. Bridge Eng.*, 10(2), 195-205.

582 NCHRP (National Cooperative Highway Research Program). (2012). *Fatigue evaluation of steel*
583 *bridges*. Report 721/2012.

584 Orcesi, A., Feraille, A., and Chataigner, S. (2019). “Fatigue strengthening of steel structures using high
585 modulus CFRP plates: development of a life-cycle analysis approach”. *Constr Build. Mat.,* 227, article
586 116628.

587 Palmer, T. (2014). *The development of welded steel fatigue design guidelines*. Taylor Machine Works.
588 Mach Des.

589 Peiris, A., and Harik, I. (2015). “Steel bridge girder strengthening using postinstalled shear connectors
590 and UHM CFRP laminates”. *J. Perform. Constr. Facil.*, 29(5): 04014139, 11 p.

591 Schnerch, D., Dawood, M., and Rizkalla, S. (2007). *Design guidelines for the use of HM strips:*
592 *strengthening of steel concrete composite bridges with high modulus carbon fiber reinforced polymer*
593 *(CFRP) strips*. North Carolina State University.

594 Tavakkolizadeh, and M., Saadatmanesh, H. (2003). “Fatigue strength of steel girders strengthened with
595 carbon fiber reinforced polymer patch”. *J. Struct. Eng.*, 129(2), 186–96.

UNE (Spanish Standardization Association). (1981). “Steel-welded fabric for concrete-reinforcing”. *UNE 36092:1981*.

UNE (Spanish Standardization Association). (2006). “Hot rolled products of structural steels – Part 2: Technical delivery conditions for non-alloy structural steels”. *UNE EN 10025-2:2006*.

UNE (Spanish Standardization Association). (2011). “Non-destructive testing of welds – ultrasonic testing – acceptance criteria”. *UNE EN ISO 11666:2011*.

UNE (Spanish Standardization Association). (2014). “Welding-fusion-welded joints in steel, nickel, titanium and their alloys (beam welding excluded) – quality levels for imperfections”. *UNE EN ISO 5817:2014*.

Wabeh, M., Boundouki, R., Schulte, C., Chataigner, S., Garcia, D., Calderon, I., Demignani, G., Martin, E., Sopena, L., and Birtel, V. (2018 a). “FASSTBridge methodology and strengthening system”. *Proceedings of TRA*, Vienna, Austria.

Wabeh, M., Boundouki, R., Weidemueller, M., Chataigner, S., Martin, E., and Sopena, L. (2018 b). “Increasing the remaining fatigue service life of steel structures using adhesively bonded composites – Design approach developed in FASSTbridge”. *Proceedings of the 9th International Conference on FRP composites in civil Engineering - CICE 2018*, Paris, part 2, 325-31.

Ye, X.W., Su, Y.H., and Han Han, J.P. (2014). “A state-of-the-art review on fatigue life assessment of steel bridges”. *Math. Problem Eng.*, article ID 956473.

Zhao, X.L., and Zhang, L. (2007). “State-of-the-art review on FRP strengthened steel structures“. *Eng. Struct.*, 9(8), 1808-23.

Zhao, X.L. (2013). *FRP-strengthened metallic structures*. CRC Press, Boca Raton, FL.

Fig. 1. General layout of the Jarama Bridge (dimensions in m)

Fig.2. General views of Jarama Bridge

Fig. 3. Location of the selected butt-weld splices for CFRP strengthening (dimensions in m)

Fig. 4. Flowchart demonstrating the different components of fatigue assessment questionnaire

Fig. 5. CFRP strengthening configurations for the six studied locations (dimensions in m)

Fig. 6. a) Application of the adhesive on the plate. b) Pressure application with rollers.

Fig.7. Pictures of the heating system used for post-curing operation

Fig. 8. Picture of a pair of strain gauges installed on the bridge

Fig. 9. Picture of the debonding sensor applied on the edge before application of the adhesive

Fig. 10. The three studied static positions on the bridge during the load tests (circles correspond to the studied butt weld locations)

Fig. 11. The two studied dynamic positions on the bridge during the load tests (circles correspond to the studied butt weld locations, vertical arrow corresponds to the position of the wooden plank)

Fig. 12. Data recorded during the placement of the two trucks on the right lane in the first static position before the strengthening intervention

Fig. 13. Data recorded during the dynamic load tests on the right lane before the strengthening intervention

Fig. 14. Summary of the average strain measurements carried out before and after reinforcement for both static and dynamic tests, at the six studied locations close to the weld toe (80 mm)

Table 1. Summary of in-shop and on-site butt-welded splices in the main girders of the Jarama Bridge

Weld N°	Span	Beam	Weld			
			Element	Distance from support, in m	Site/Workshop	Status
31	1	1 (length: 16.88 m)	Bottom flange butt weld	2.06	Workshop	Fulfills
30	1	1 (length: 16.88 m)	Bottom flange butt weld	9.44	Workshop	DOES NOT fulfill
23	1	2 (length: 16.88 m)	Bottom flange butt weld	8.08	Workshop	DOES NOT fulfil
22	1	2 (length: 16.88 m)	Bottom flange butt weld	14.08	Workshop	DOES NOT fulfil
29	2	1 (length: 23.94 m)	Bottom flange butt weld	6.11	Workshop	Fulfills
28	2	1 (length: 23.94 m)	Bottom flange butt weld	10.67	Workshop	Fulfills
27	2	1 (length: 23.94 m)	Bottom flange butt weld and web butt weld (lowerpart)	12.78	Site	DOES NOT fulfil
26	2	1 (length: 23.94 m)	Bottom flange butt weld	16.34	Workshop	Fulfills
25	2	1 (length: 23.94 m)	Bottom flange butt weld	20.04	Workshop	Fulfills
24	2	1 (length: 23.94 m)	Bottom flange butt weld	23.01	Workshop	DOES NOT fulfil
21	2	2 (length: 23.94 m)	Bottom flange butt weld	1.3	Workshop	DOES NOT fulfil
20	2	2 (length: 23.94 m)	Bottom flange butt weld	7.84	Workshop	Fulfills
19	2	2 (length: 23.94 m)	Bottom flange butt weld	12.41	Workshop	Fulfills
18	2	2 (length: 23.94 m)	Bottom flange butt weld and web butt weld (lowerpart)	14.41	Site	DOES NOT fulfill
17	2	2 (length: 23.94 m)	Bottom flange butt weld	17.14	Workshop	Fulfills
16	2	2 (length: 23.94 m)	Bottom flange butt weld	19.94	Workshop	Fulfills
15	2	2 (length: 23.94 m)	Bottom flange butt weld	22.98	Workshop	Fulfills
6	4	1 (length: 23.88 m)	Bottom flange butt weld	1.05	Workshop	DOES NOT fulfil
7	4	1 (length: 23.88 m)	Bottom flange butt weld	3.08	Workshop	Fulfills
8	4	1 (length: 23.88 m)	Bottom flange butt weld	6.44	Workshop	Fulfills
9	4	1 (length: 23.88 m)	Bottom flange butt weld and web butt weld (lowerpart)	11.35	Site	DOES NOT fulfill
10	4	1 (length: 23.88 m)	Bottom flange butt weld	16.95	Workshop	Fulfills
11	4	1 (length: 23.88 m)	Bottom flange butt weld	22.98	Workshop	DOES NOT fulfil
1	4	2 (length: 23.88 m)	Bottom flange butt weld	2.75	Workshop	Fulfills
2	4	2 (length: 23.88 m)	Bottom flange butt weld	5.86	Workshop	Fulfills
3	4	2 (length: 23.88 m)	Bottom flange butt weld and web butt weld (lowerpart)	9.57	Site	DOES NOT fulfill
4	4	2 (length: 23.88 m)	Bottom flange butt weld	14.68	Workshop	DOES NOT fulfil
5	4	2 (length: 23.88 m)	Bottom flange butt weld	20.14	Workshop	DOES NOT fulfil
14	5	1 (length: 16.63 m)	Bottom flange butt weld	8.18	Workshop	DOES NOT fulfil
12	5	2 (length: 16.63 m)	Bottom flange butt weld	6.08	Workshop	DOES NOT fulfill
13	5	2 (length: 16.63 m)	Bottom flange butt weld	11.99	Workshop	Fulfills

Table 2. Summary of key fatigue design variables used in FASSTbridge fatigue assessment methodology tool

Description	AASHTO	Eurocode
Fatigue loads	Live Load (*LL*), Dynamic Load (*IM*), Centrifugal Load (*CE*)	Fatigue Load Model 1, 2 or 3
Average daily traffic	*ADT*	n/a
Number of trucks in traffic	Highway classification (*h*)	Traffic category based on N_{obs} /per year (λ_2)
Average daily truck traffic	*ADTT* (=*ADT* x *h*)	Traffic type
Fraction of truck traffic in a single lane	Number of lanes available to trucks (*p*)	Number of slow lanes
Truck traffic in a single lane	$ADTT_{SL}$ (=*ADTT* x *p*) / per day	N_{obs} /per year
Stress range from truck passage	Cycles per truck passage (*n*)	Damage effect of traffic (λ_f)
Detail design constant	Detail category (*A*)	Detail category (*CAFT* for *N*= 2000000)
Stress range cycles over design life	Number of cycles (*N*)	Number of cycles (*N*)
Recommended design life	75 years	100 years

Table 3. Proposed modification factors (α values) used for the (a) AASHTO and (b) Eurocode fatigue assessment and remaining fatigue life calculations.

a_n	AASHTO	Eurocode
a_1	A: design detail fatigue resistance	$\Delta\sigma_c$: design detail fatigue resistance
a_2	N: number of stress range cycles	γ_{Mf}: partial factor for fatigue strength
a_3	ADT: average daily traffic	λ_1:damage effect of traffic
a_4	p: single lane	N_{obs}: single lane truck traffic
a_5	Single lane truck traffic	λ_2: expected annual traffic volume
a_6	$[(\Delta f)_{eff}]^3$: fatigue load stress range	γ_{Ff}: safety factor for fatigue loading
a_7	Girder type, effects of corrosion, level of importance, risk tolerance, etc …	$\Delta\sigma_{FLM3}$: fatigue load stress range

Table 4. Remaining fatigue life of studied assembly at the Jarama Bridge

Weld No	Weld Code	Remaining service life
29	S2-B1-W1	> 100 years
26	S2-B1-W4	> 100 years
25	S2-B1-W5	> 100 years
20	S2-B2-W2	40 - 50 years
17	S2-B2-W5	> 100 years
16	S2-B2-W6	> 100 years

Table 5: Strengthening configuration used in selected welds.

Weld No.	Weld code	Number of laminates	Number of layers	Length [mm]		
				Layer 1	Layer 2	Layer 3
29	S2-B1-W1	4	2	1400	1200	-
26	S2-B1-W4	5	1	1200	-	-
25	S2-B1-W5	3	3	1600	1400	1200
20	S2-B2-W2	4	2	1400	1200	-
17	S2-B2-W5	5	1	1200	-	-
16	S2-B2-W6	3	3	1600	1400	1200

Table 6. Estimated remaining fatigue life of specific joints at the Jarama Bridge, before and after strengthening

Weld No.	Weld code	Remaining Fatigue Life (years)	
		Unstrengthened Girders	CFRP Strengthened Girders
29	S2-B1-W1	> 100 years	> 100 years
26	S2-B1-W4	> 100 years	> 100 years
25	S2-B1-W5	> 100 years	> 100 years
20	S2-B2-W2	40 - 50 years	120 - 130 years
17	S2-B2-W5	> 100 years	> 100 years
16	S2-B2-W6	> 100 years	> 100 years

Table 7. Maximum measured differential strains before and after reinforcement for static and dynamic load tests and for the six studied locations close to the weld toe (80 mm)

Sensor	Laminates	Static before	Static after	Difference	Dynamic before	Dynamic after	Difference
29-1	2 x 4 (8)	77 με	58 με	- 25 %	71 με	51 με	- 28 %
26-1	1 x 5 (5)	84 με	67 με	- 20 %	84 με	77 με	- 8 %
25-1	3 x 3 (9)	69 με	51 με	- 26 %	65 με	53 με	- 18 %
20-1	2 x 4 (8)	84 με	59 με	- 30 %	80 με	56 με	- 30 %
17-1	1 x 5 (5)	68 με	56 με	- 18 %	75 με	62 με	- 17 %
16-1	3 x 3 (9)	71 με	56 με	- 21 %	60 με	45 με	- 25 %

Table 8. Maximum measured differential strains before and after reinforcement for static and dynamic load tests and for the six studied locations far from the weld toe (950 mm)

Sensor	Laminates	Static before	Static after	Difference	Dynamic before	Dynamic after	Difference
29-2	2 x 4 (8)	71 με	63 με	- 11 %	64 με	61 με	- 5 %
26-2	1 x 5 (5)	85 με	72 με	- 15 %	91 με	88 με	- 3 %
25-2	3 x 3 (9)	63 με	55 με	- 13 %	60 με	55 με	- 8 %
20-2	2 x 4 (8)	77 με	66 με	- 14 %	74 με	62 με	- 16 %
17-2	1 x 5 (5)	82 με	71 με	- 13 %	92 με	80 με	- 13 %
16-2	3 x 3 (9)	69 με	59 με	- 14 %	60 με	52 με	- 13 %

Figure 1

Click here to access/download;Figure;Figure1.tif

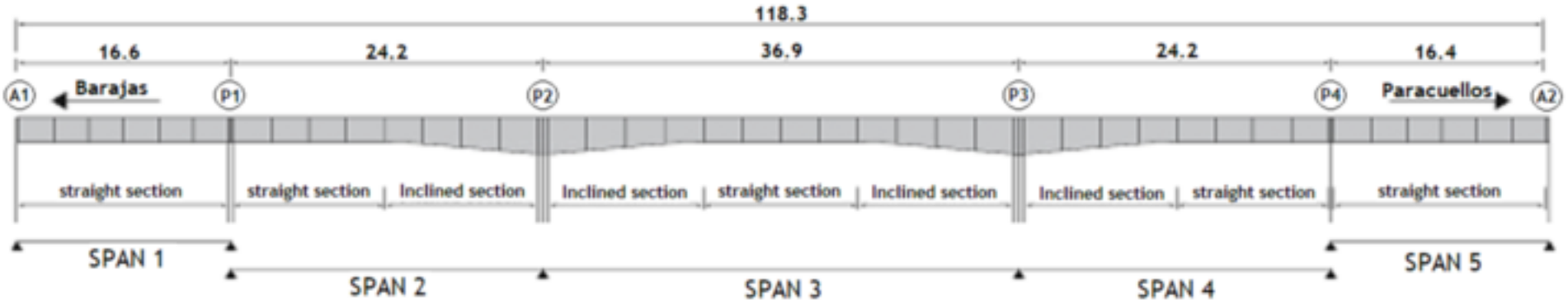

Figure 2

Figure 3

Click here to access/download;Figure;Figure3.tif

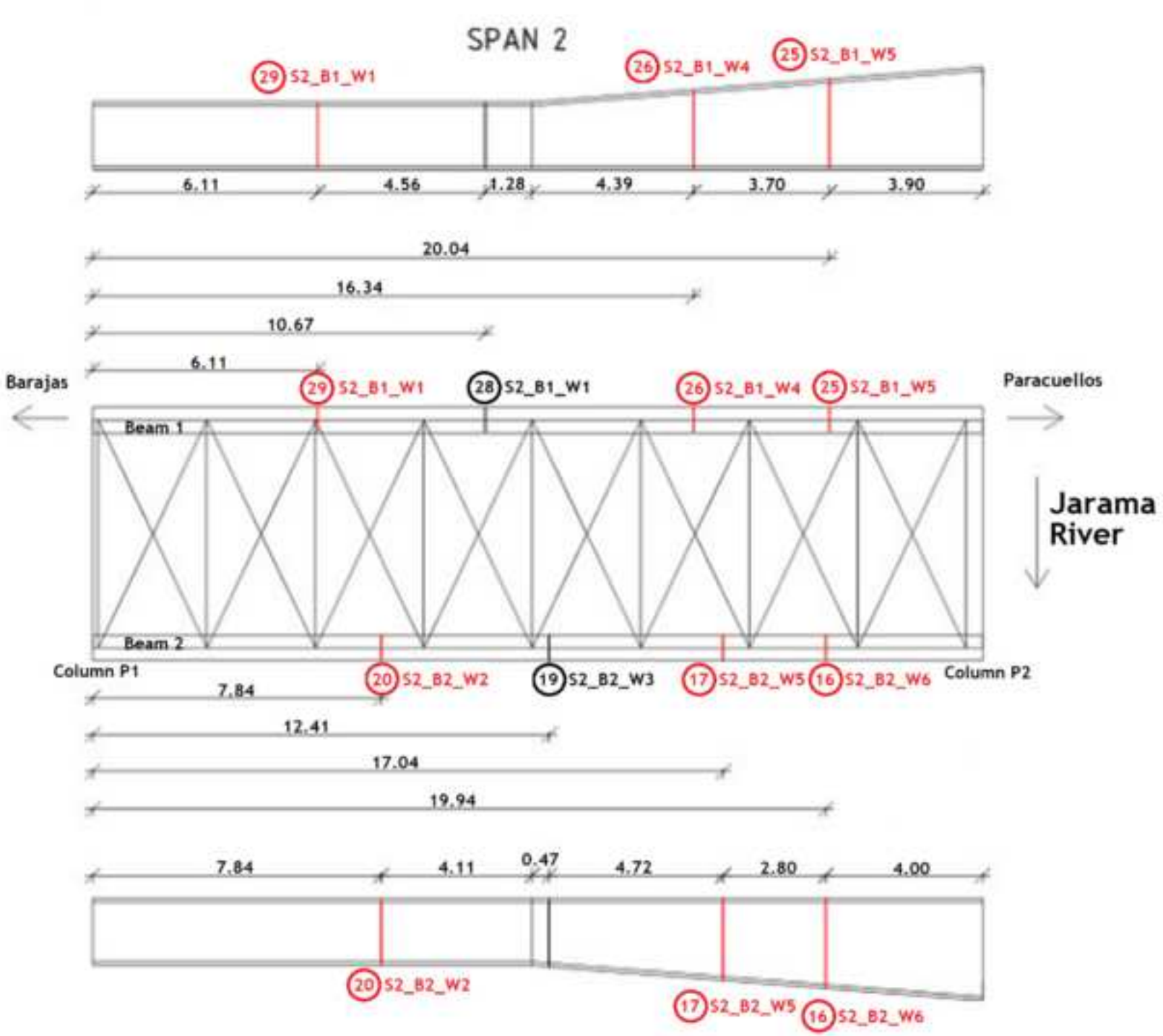

Figure 4

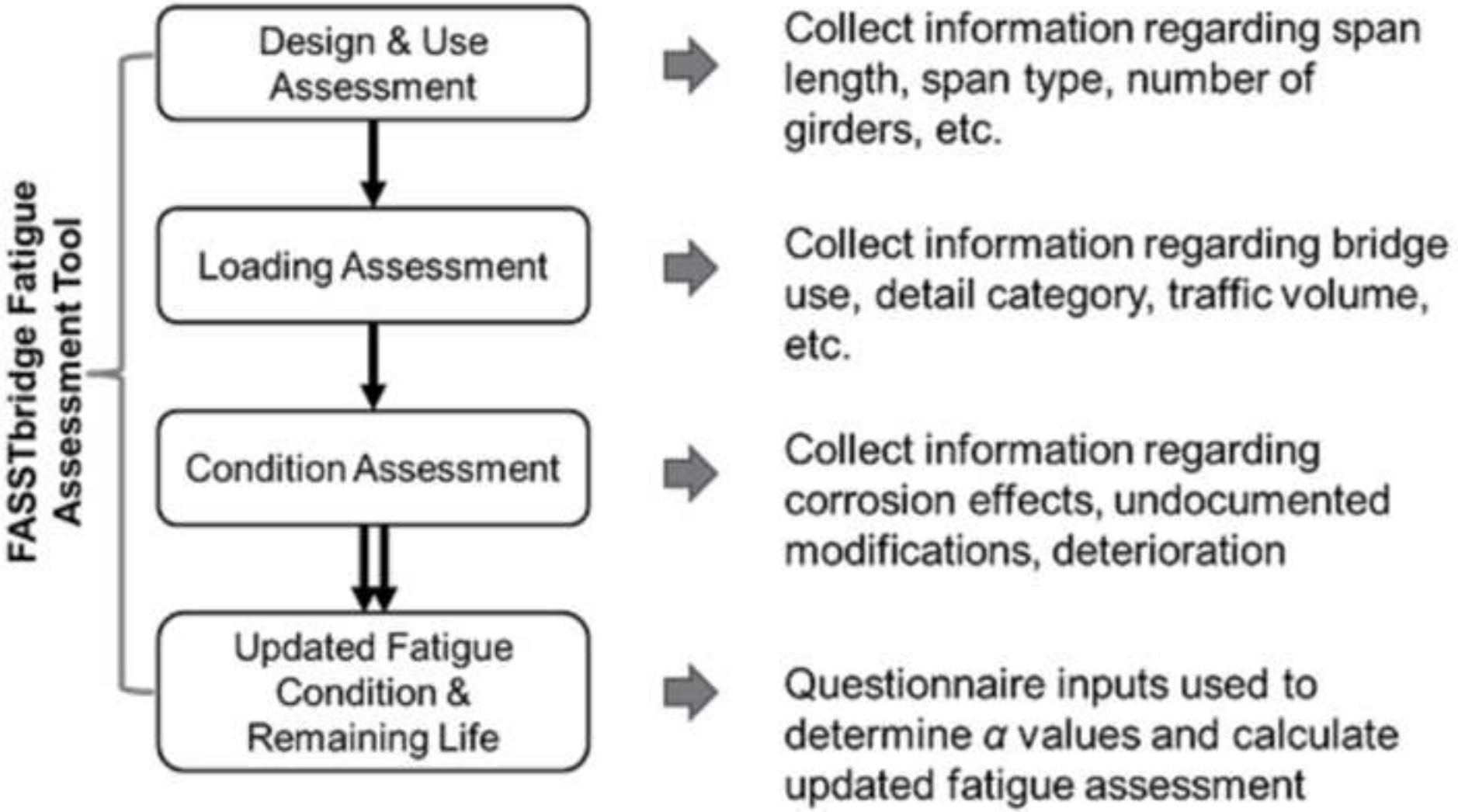

Figure 5

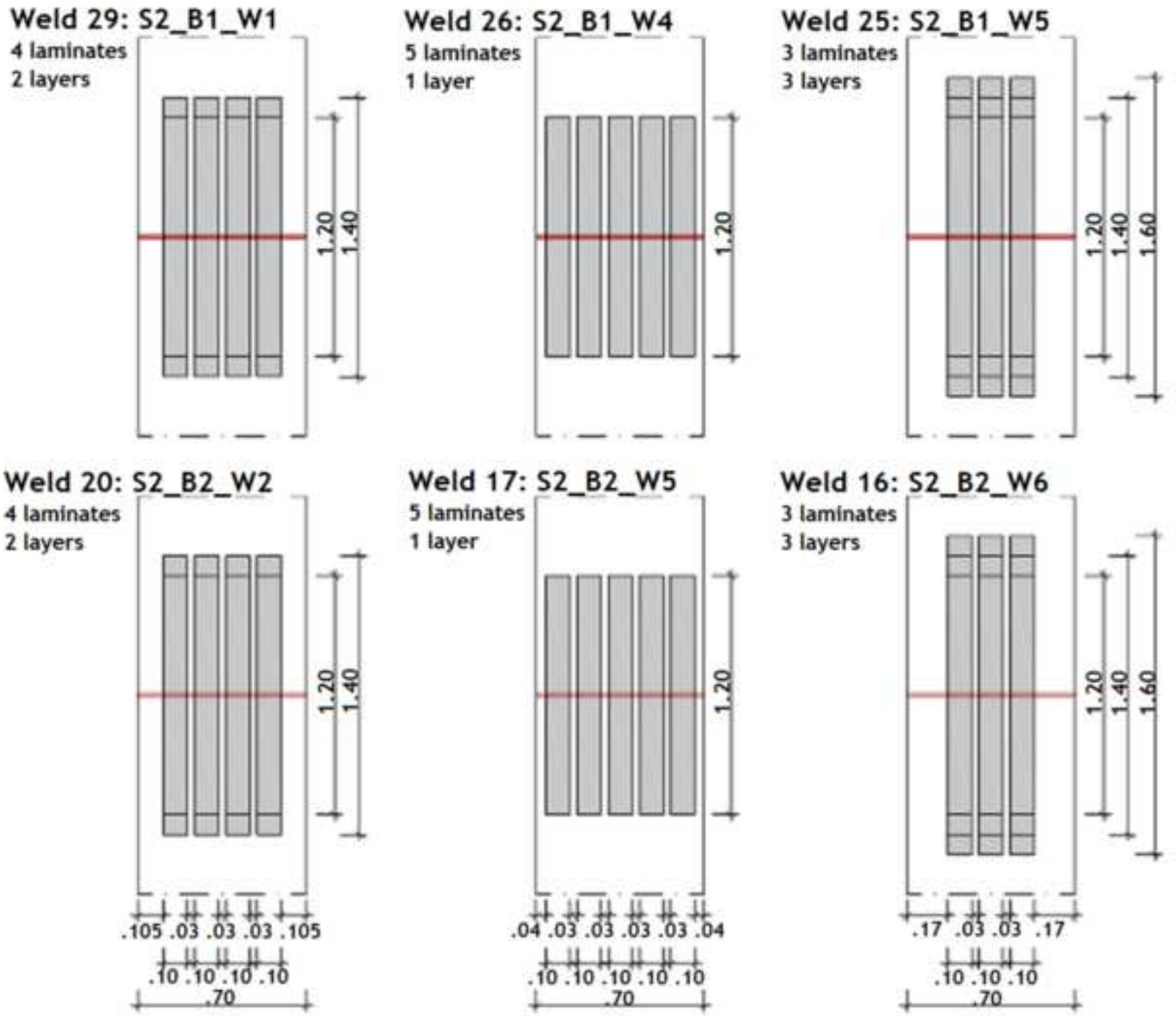

Figure 6

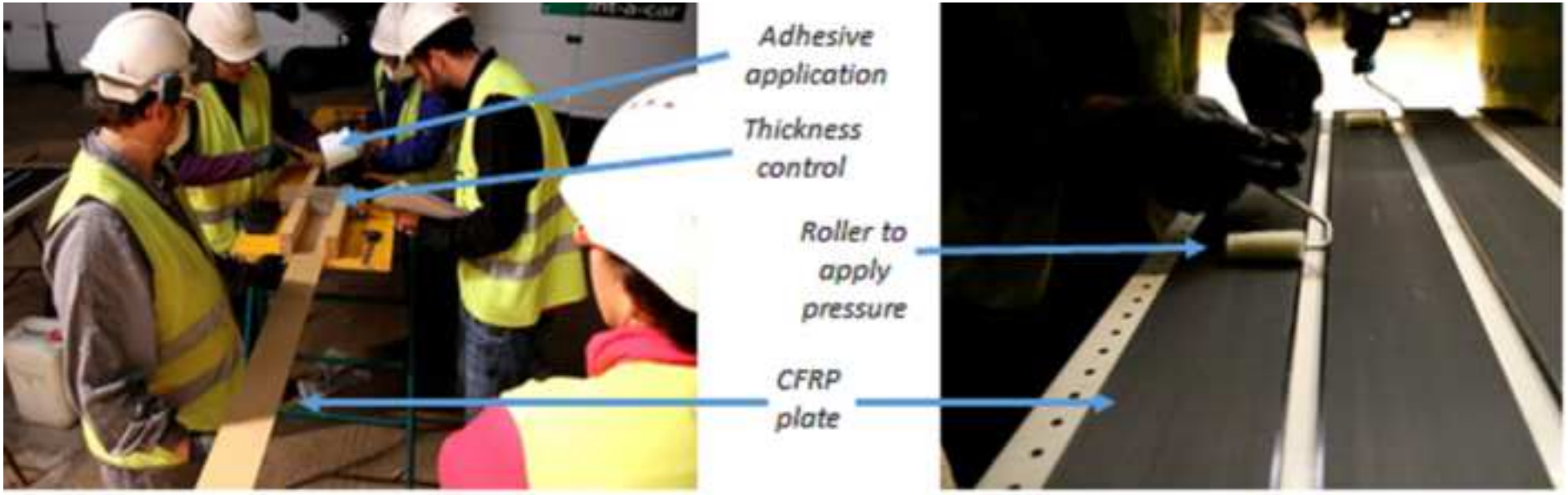

Figure 7

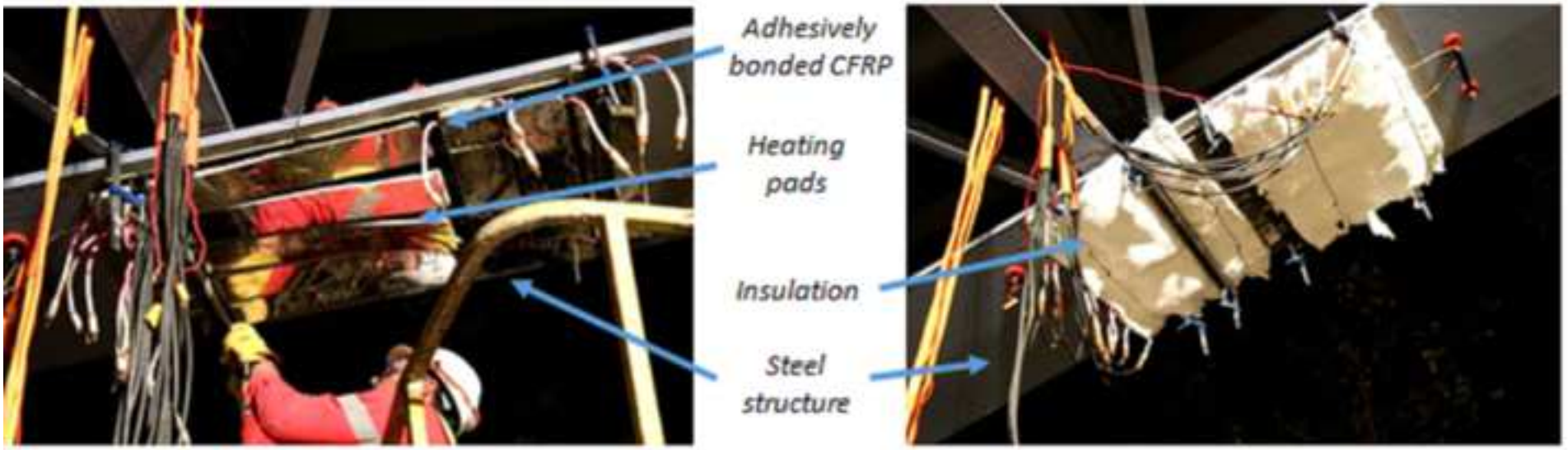

Figure 8

Click here to access/download;Figure;Figure8.tif

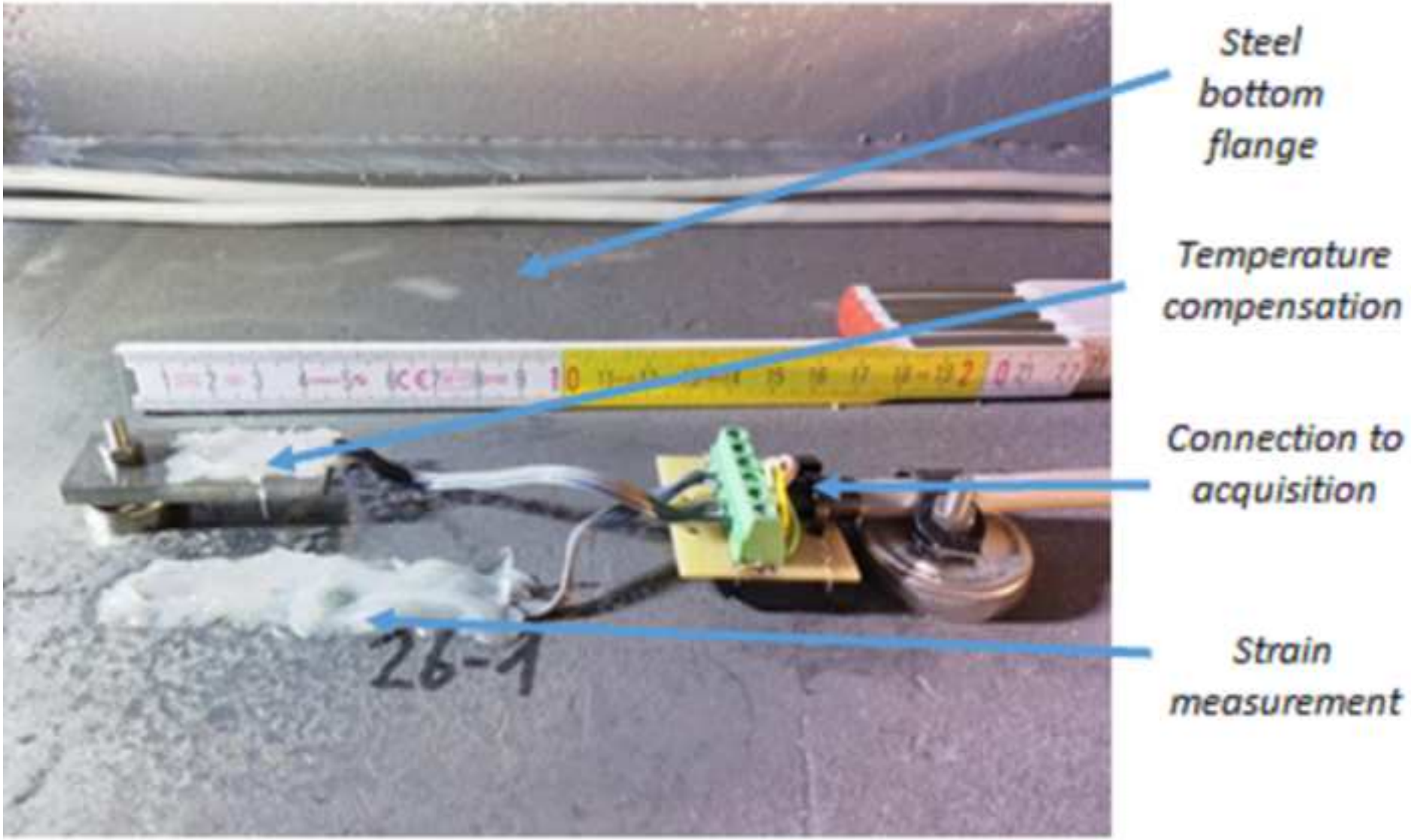

Figure 9

Click here to access/download;Figure;Figure9.tif

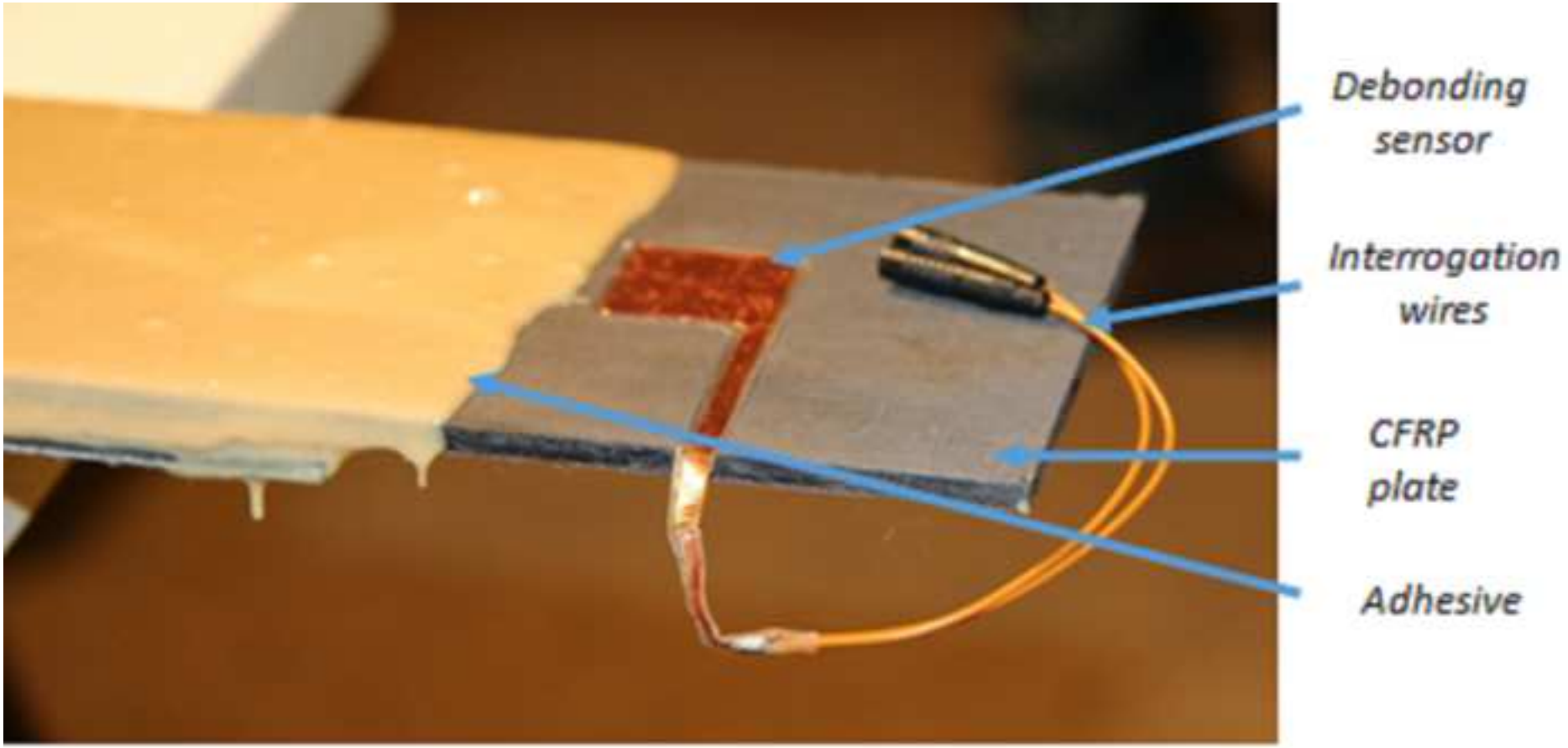

Figure 10

Click here to access/download;Figure;Figure10.tif

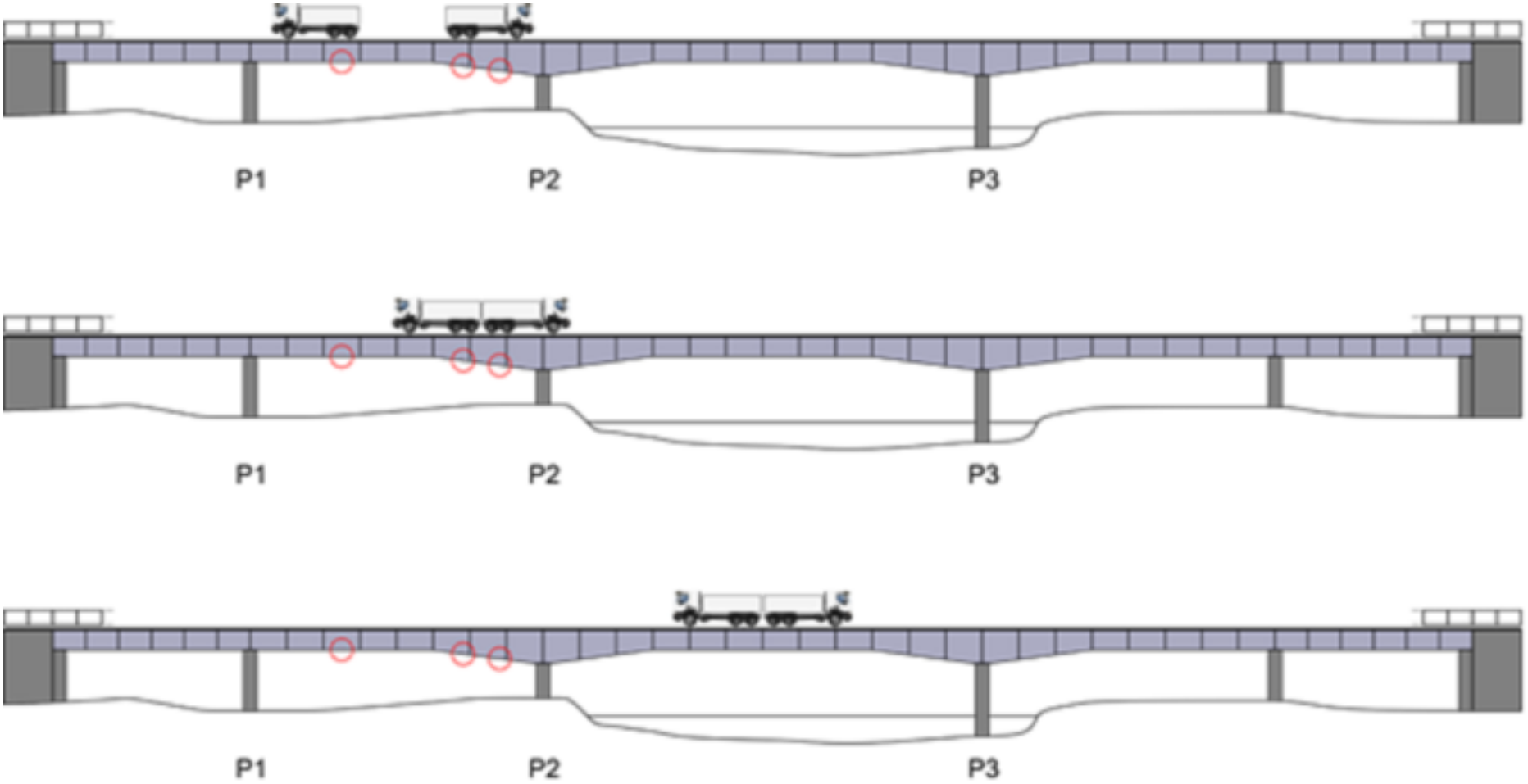

Figure 11

Click here to access/download;Figure;Figure11.tif

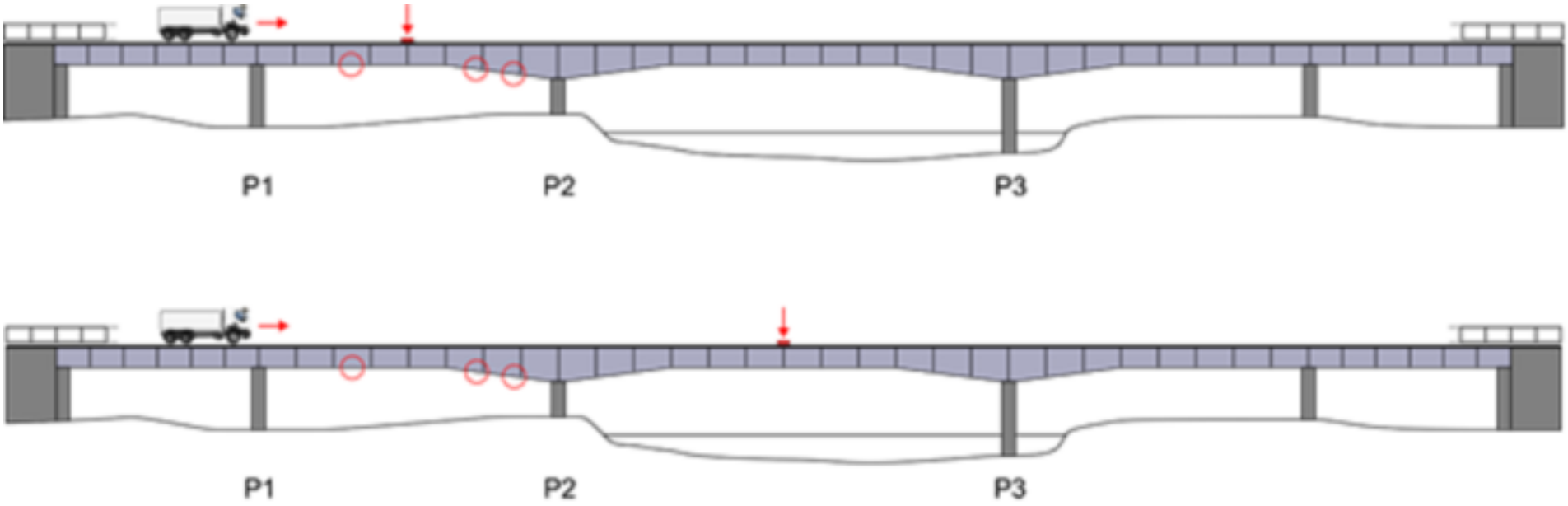

Figure 12

Click here to access/download;Figure;Figure12.tif

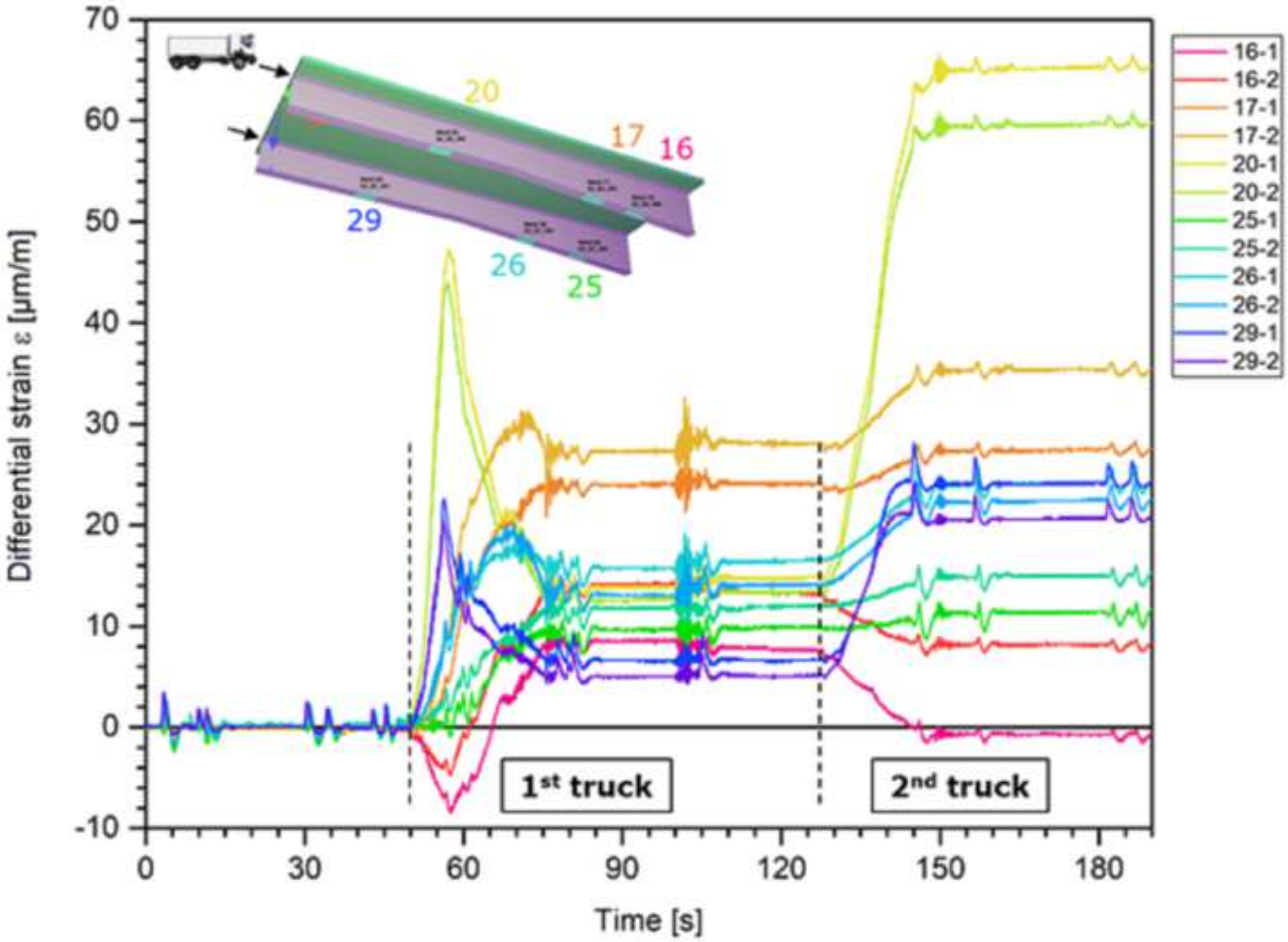

Figure 13

Click here to access/download;Figure;Figure13.tif

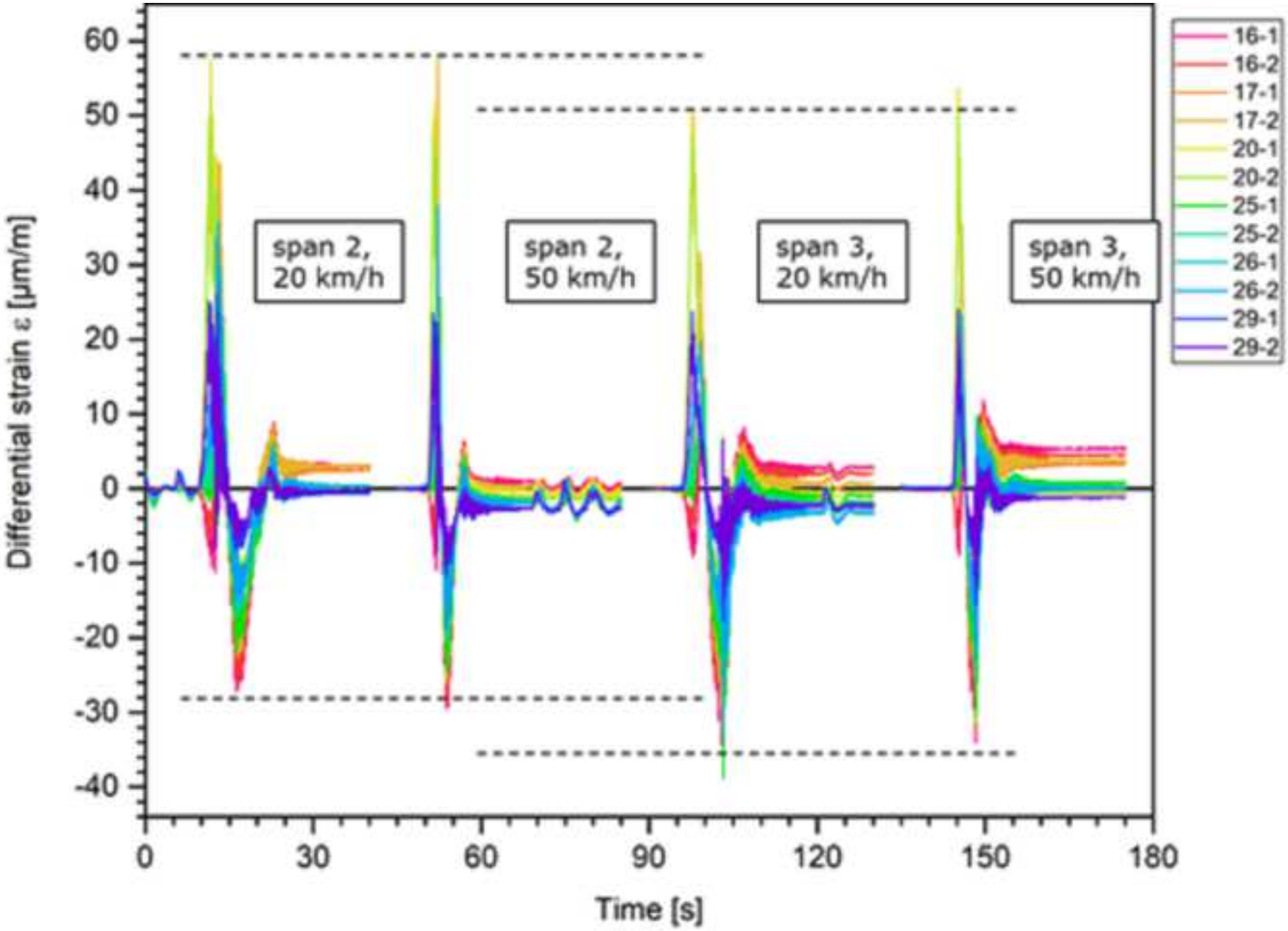

Figure 14